# Modal Behavior of Dominant Modes on Gyromagnetic Asymmetric Coupled Lines in Both Leaky and Nonradiation Regions

Kuen-Fwu Fuh, Ching-Kuang C. Tzuang, Chien-Chang Liu and Yu-Cheng Lin

Institute of Electrical Communication Engineering, National Chiao Tung University
No. 1001, Ta Hsueh Road, Hsinchu, Taiwan, ROC

## Abstract

By employing rigorous full-wave spectral domain approach, the complex propagation constants of the dominant modes on gyromagnetic asymmetric coupled lines are shown to support both complex modes and leaky modes. As one gradually increases the dielectric loading of the gyromagnetic lines, the transformation of dominant complex modes into a pair of a forward leaky mode and a backward leaky mode is observed. All the dominant modes reported here have been verified by examining their corresponding transverse field plots.

## I. Introduction

Microwave circuits employing complex waves have found various applications such as active integrated antenna and sensors [1,2]. One example showing how to apply the higher-order leaky mode for a quasi-planar integrated leaky wave antenna design had been reported recently [3]. There are many papers discussing the leaky modes on a number of planar and quasi-planar guided wave structures, e.g., references [4-10], to name a few. This paper, however, will report the complex waves arising from the *dominant modes* in the form of complex modes and leaky modes. To authors' best knowledge, the complex modes in open planar waveguides have never been found except for the open stratified dielectric or ferrite-loaded parallel-plate waveguides [11,12]. The complex modes investigated here also evolve to leaky modes when the dielectric loading is increased.

Fig. 1 depicts the waveguide model under analysis. It consists of two coupled lines sandwiched between a dielectric slab of thickness $h_1$ and a ferrite substrate of thickness $h_2$, a bottom metallic plate and a top cover. The ferrite substrate is magnetized perpendicularly along x direction. Section II will briefly describe the rigorous spectral domain approach employing the dyadic Green's impedance function. Section III discusses the modal solutions of Fig. 1 with one set of structure and material constants. The transverse vector field plots of Section IV are used to verify our theoretic results. Section V concludes the important results.

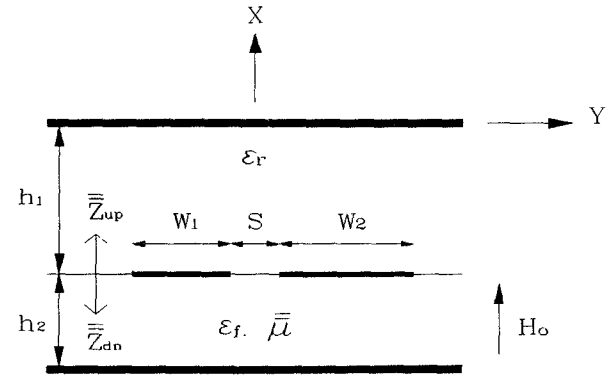


Fig. 1 Cross-sectional view of ferrite-loaded asymmetric coupled strips with dielectric region (layer 1) height = $h_1$, ferrite substrate (layer 2) height = $h_2$, gap = S, strip widths $W_1$ and $W_2$, ferrite saturation magnetization = Ms, and ferrite bias field = Ho.

## II. Full-Wave Analysis

The small-signal magnetic property of a magnetized ferrite medium is characterized by a permeability tensor. In the following, $\mu$ and $\kappa$ represent the diagonal and off-diagonal elements of the permeability tensor, respectively. Referring to Fig. 1, the eigen wave numbers of the two sets of hybrid EH and HE spectral waves in the ferrite substrate along the x-direction are

TH 3F



0-7803-3246-6/96/$5.00 © IEEE

$$\lambda^2_{he,eh} = (\lambda_h^2 + \lambda_e^2)/2 \pm \sqrt{\left(\lambda_h^2 - \lambda_e^2\right)^2/4 - k_o^2 \varepsilon_f \lambda_h^2 \kappa^2/\mu} \quad (1)$$

where $\lambda_h$ and $\lambda_e$ are the wave numbers of the TE and the TM spectral waves, respectively, with respect to the distinguished (x) axis in the magnetic uniaxial media ($\kappa$=0) [13]. Equation (1) has the conventional form of coupled-mode formulas and it indicates that TE and TM waves couple in ferrite media due to the effect of non-vanishing $\kappa$. After certain algebraic manipulations in the spectra domain, the tangential electric $\tilde{\bar{E}}_T = \left[\tilde{E}_t \cdot \hat{x} \times \hat{k}_t, \tilde{E}_t \cdot \hat{k}_t\right]^T$ and magnetic $\tilde{\bar{H}}_T = \left[\tilde{H}_t \cdot -\hat{k}_t, \tilde{H}_t \cdot \hat{x} \times \hat{k}_t\right]^T$ fields at the lower (+) and upper (-) interfaces of the ferrite medium are related by the following forms:

$$\begin{bmatrix} \tilde{\bar{E}}_T \\ \tilde{\bar{E}}_T \end{bmatrix}_{4\times 1} = \begin{bmatrix} \bar{\bar{Z}}_{11} & \bar{\bar{Z}}_{12} \\ \bar{\bar{Z}}_{21} & \bar{\bar{Z}}_{22} \end{bmatrix}_{4\times 4} \begin{bmatrix} \tilde{\bar{H}}_T \\ -\tilde{\bar{H}}_T \end{bmatrix}_{4\times 1} \quad (2)$$

where $\hat{k}_t$ is the unit vector in the direction of the transverse propagation vector of the spectral wave. The two by two matrix $\bar{\bar{Z}}_{11} (= \bar{\bar{Z}}_{22})$ is expressed as

$$\bar{\bar{Z}}_{11} = \begin{bmatrix} 1 & K_V^e \\ K_V^h & 1 \end{bmatrix} \begin{bmatrix} Z_h \coth(\lambda_{eh} h) & 0 \\ 0 & Z_e \coth(\lambda_{eh} h) \end{bmatrix} \begin{bmatrix} 1 & K_I^e \\ K_I^h & 1 \end{bmatrix}^{-1} \quad (3)$$

and the expression for $\bar{\bar{Z}}_{12} (= \bar{\bar{Z}}_{21})$ is obtained by replacing the hyperbolic function coth with csch in equation (3). Here, $Z_h = jk_o Z_o \mu \lambda_{he}/\lambda_h^2, Z_e = \lambda_{eh}/jk_o Y_o \varepsilon_f$ and $Z_o (= Y_o^{-1})$ is the free space wave impedance. The nonvanishing off-diagonal elements in equation (3) are

$$K_I^h = \frac{\lambda_{he}^2 - \lambda_h^2}{j\lambda_h^2 \kappa/\mu} = K_V^h \frac{k_o^2 \varepsilon_f \mu}{-\lambda_h^2}, K_I^e = \frac{\lambda_{eh}^2 - \lambda_e^2}{jk_o^2 \varepsilon_f \kappa} = K_V^e \frac{-\lambda_h^2}{k_o^2 \varepsilon_f \mu} \quad (4)$$

It can be shown that when $\kappa$=0, $K_I^h$ , $K_I^e$, $K_V^h$, and $K_V^e$ reduce to zero and the TE and the TM fields are decoupled. The ferrite medium can be reduced to isotropic dielectric medium by setting $\mu$=1 and $\kappa$=0. Therefore the formulations derived above can also be applied to the dielectric substrate of layer 1 in Fig. 1. Then the driving point impedance matrices $\bar{\bar{Z}}_{up}$ and $\bar{\bar{Z}}_{dn}$, as shown in Fig. 1, can be readily derived. By matching the last boundary conditions at the metal-strip interface, the dyadic Green's function is derived, namely,

$$\begin{bmatrix} \tilde{Z}_{zz} & \tilde{Z}_{zy} \\ \tilde{Z}_{yz} & \tilde{Z}_{yy} \end{bmatrix} = -\bar{\bar{T}} \left( \bar{\bar{Z}}_{up}^{-1} + \bar{\bar{Z}}_{dn}^{-1} \right)^{-1} \bar{\bar{T}}^{-1} \quad (5)$$

where $\bar{\bar{T}}$ is the transformation matrix that maps the $(\hat{k}_t, \hat{x} \times \hat{k}_t)$ coordinate system to the $(\hat{y}, \hat{z})$ coordinate system. Then the Galerkin's procedure is applied to derive a system of homogeneous linear equations. Finally, the propagation constants are the zeros of the determinant of the linear matrix equations after Galerkin's process.

## III. Complex Modes and Leaky Modes Arising from Dominant Modes

Given a particular case study for Fig. 1 with $h_1$=20 mm, $h_2$=2 mm, Ms=95.5 kA/m , Ho=95.5 kA/m, $W_1$=0.5 mm, $W_2$=1.5 mm and S=0.5 mm, $\varepsilon_f$=13.5, the modal characteristics against the value of the dielectric loading of layer 1 are shown in Fig. 2, where we observe two distinct regions. The working frequency of Fig. 2 is 8 GHz. Here $\beta$ and $\alpha$ denote the real and the imaginary parts of the propagation constant $k_z = \beta - j\alpha$, respectively. When the relative dielectric constant of layer one is below 11.75, two dominant modes are in the nonradiation region with $\beta_1$ and $\beta_2$ greater than $\beta_{s1}$ (the lowest order surface wave mode). An extensive numeric search for bound modes with real propagation constants has been conducted. The results are shown in Fig. 2, where only the region with $\varepsilon_r$ lying between 6.20 and 6.806 can two real propagating modes exist. These two propagating bound modes are so close to each other that their transverse field patterns worth investigating while we expect they would possess certain field characteristics that appear in the well-known C-mode and $\pi$-mode of the asymmetric coupled lines on isotropic dielectric substrates. This will be discussed in the next section. Clearly the nonradiation region is also the complex modes region established by the mode-coupling of the two dominant modes as the result of both ferrite and dielectric loading on the coupled lines. The complex propagation constants are complex conjugated like those obtained for the shielded lossless nonreciprocal finline [14].

When $\varepsilon_r$ is above 11.75, the mode conversion takes place. As shown in Fig. 2, the complex modes transform to a pair of a forward leaky mode and a backward leaky mode. In other words, the spectral complex modes split into leaky modes, which are not a complex conjugate pair. Although all the material

constants are assumed to be free of loss, the waveguide now is lossy in a sense that forward leaky mode radiates and carries electromagnetic energy away from the waveguide. The forward leaky mode is improper wave with $\beta_{FL}>0$ and $\alpha_{FL}>0$ and attenuates along positive z-axis while radiating laterally the energy as it travels. The backward leaky mode is a proper wave with $\beta_{BL}>0$ and $\alpha_{BL}<0$ and its field decays in the transverse plane [15]. Such mode-splitting process is the second of its kind known to date. The first example is a pair of forward leaky modes that are coupled to form a new pair of a forward leaky mode and a backward leaky mode in a partially-open gyromagnetic slotline [9]. Notice that the forward leaky-mode solutions jump at crossing the surface waves solutions. This is the direct result of including the contribution of the surface wave poles above cutoff in the SDA formulation. Such modal jump had been reported by Marques et. al. [16]. However the backward leaky mode suffers no such jump in the leaky region.

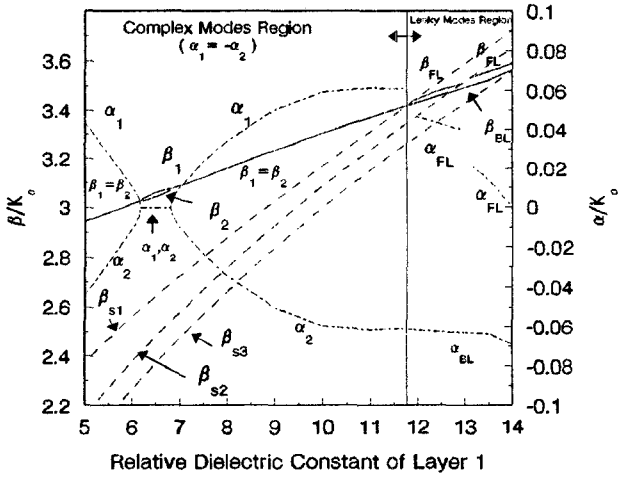


Fig. 2 The complex propagation constants of the two dominant modes against the dielectric loading of layer 1 of Fig. 1. The working frequency is 8 GHz and the material and structural constants are listed in the context. The solid (dash-dot) lines are for the real (imaginary) parts of the complex propagation constants. The dashed lines represent the surface wave modes.

## IV. Transverse Field Plots of Dominant Modes

Although our extensive roots search has shown that the bound (non-leaky) dominant modes occupy almost all the nonradiation region as shown in Fig. 2, the most direct proof of such claim, however, lies in the transverse field plots of the dominant modes. Fig. 3 and Fig. 4 plot the transverse electric vector fields near the asymmetric coupled lines for the two dominant modes of real propagation constants $\beta_1$ and $\beta_2$ located at $\varepsilon_r = 6.8$ of Fig. 2, respectively. They show strikingly similar transverse field patterns and tend to couple each other, resulting in the formation of complex modes for most nonradiation region [14]. By taking careful observation, we can found that the transverse field distribution of Fig. 3 in the ferrite region resembles those of the isotropic C mode but significantly distorted in the region underneath the narrow strip and gap. On the other hand, the transverse field distribution of Fig. 4 resembles those of the isotropic $\pi$ mode and more significant distortion is found in the side of narrow strip. Thereby these two propagating modes $\beta_1$ and $\beta_2$ are indeed bound dominant modes lying in the nonradiation region. The differences between the field patterns of gyromagnetic dominant modes and those of the isotropic C mode and $\pi$ mode can be contributed to the field-displacement effect of ferrite-loading and the strong coupling mechanism.

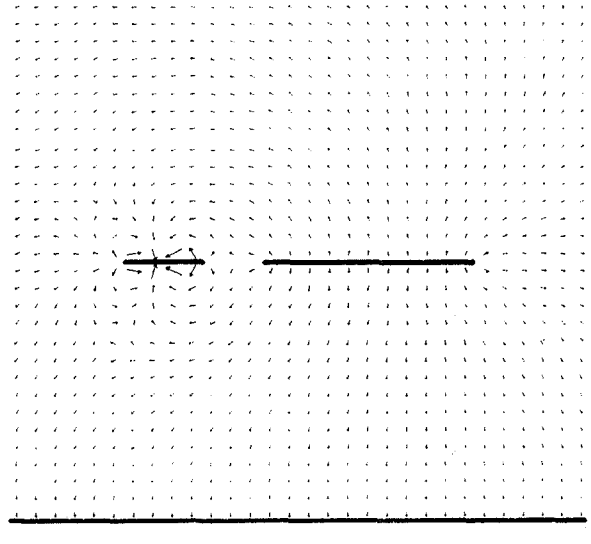

Fig. 3 The transverse electric vector fields of the dominant mode with real normalized propagation constant $\beta_1$=3.075 as shown in Fig. 2 at $\varepsilon_r$=6.8.

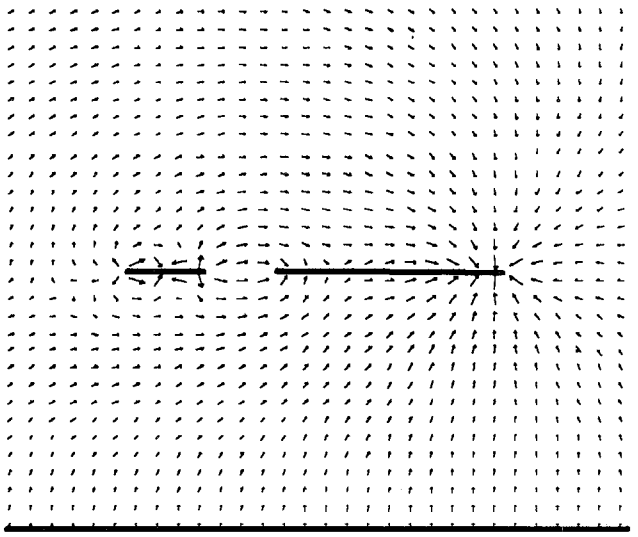

Fig. 4 The transverse electric vector fields of the dominant mode with real normalized propagation constant $\beta_2$=3.071 as shown in Fig. 2 at $\varepsilon_r$=6.8.

## V. Conclusion

Rigorous spectral-domain formulation for obtaining the propagation characteristics of planar or quasi-planar waveguides shows that the dominant modes can be complex waves in the form of complex modes or leaky modes for one case study, in which the guided structures consist of two asymmetric coupled lines sandwiched in a dielectric slab and a perpendicularly magnetized ferrite substrate. Detailed transverse electric vector field plots also illustrate that the modes reported in the paper are dominant modes. The leaky modes converted from complex modes can be controlled by changing the dielectric loading of the guided structure. When this occurs, a pair of a forward leaky mode and a backward leaky mode is found. The former represents radiation loss whereas the latter is a proper mode. Therefore the solutions in this leaky domain are no longer complex conjugate.

## Acknowledgment

This work was supported in part by the National Science Council, Taiwan, ROC, under Grant A85042 and NSC85-2213-E009-003

## References

[1] C.-K. C. Tzuang and G.-J. Chou, "An active microstrip leaky-wave antenna employing uniplanar oscillator," *25th European Microwave Conference*, pp.308-311.

[2] C.-K. C. Tzuang, S.-P. Liu and G.-J. Chou, "Integrated active leaky-wave antenna employing arched microstrip line," *1995 Asia-Pacific Microwave Conference Proceedings*, pp. 335-338.

[3] G.-J. Chou and C.-K. C. Tzuang, "An integrated leaky-wave antenna," accept for publication on *IEEE Transaction on Antenna and Propagation.*

[4] L. Carin, "Leakage effects in broadside-coupled microstrip," *IEEE MTT-S Int. Microwave Symp. Dig.*, pp. 559-562, 1991.

[5] D. Nghien, J. T. Williams, D. R. Jackson, and A. A. Oliner, "Proper and Improper modal solutions for inhomogeneous stripline," *IEEE MTT-S Int. Microwave Symp. Dig.*, pp. 567-570, 1991.

[6] M. Tsuji, H. Shigesawa, and A. A. Oliner, "Printed-circuit waveguides with anisotropic substrates: a new leakage effect," *IEEE MTT-S Int. Microwave Symp. Dig.*, pp. 783-786,1989.

[7] Y. Liu and T. Itoh, "Leakage phenomena in multi-layered conductor-backed coplanar waveguides," *IEEE Microwave and Guided Wave Letters*, vol. 3, no. 11, Nov. 1993.

[8] Y. D. Lin and Y. B. Tsai, "Surface Wave Leakage Phenomena in Coupled Slot Lines," *IEEE Microwave and Guided Wave Letters*, vol. 4. no. 10, Oct. 1994.

[9] K.-F. Fuh and C.-K. C. Tzuang, "The effect of covering on complex wave propagation in gyromagnetic slotlines," *IEEE Transaction on Microwave Theory and Techniques*, vol. 43, No. 5, pp. 1100-1105, May 1995.

[10] K.-F. Fuh and C.-K. C. Tzuang, "Magnetically scannable microstrip antenna employing a leaky gyromagnetic microstrip line," *Electronics Letters*, 3rd August 1995, Vol. 31, No. 16, pp. 1309-1310.

[11] T. Tamir and A. A. Oliner, "Guided complex waves," *Proc. IEE*, vol. 110, no. 2, pp. 310-334, February 1963.

[12] R. Marques, F. L. Mesa, and M. Horno, "Nonreciprocal and reciprocal complex and backward waves in parallel plate waveguides loaded with a ferrite slab arbitrarily magnetized," *IEEE Transaction on Microwave Theory and Techniques*, vol. 41, no. 8, pp. 1409-1418, August 1993.

[13] S. Przezdziecki and R. A. Hurd, "A note on scalar Hertz potentials for gyrotropic media," *Appl. Phys.*, vol. 20, pp. 313-317, 1979.

[14] C.-K. C. Tzuang and J.-M. Lin, "On the mode-coupling formation of complex modes in a nonreciprocal finline," *IEEE Transaction on Microwave Theory and Techniques*, vol. 41, no. 8, pp. 1400-1408, August 1993.

[15] A. Ishimaru, *Electromagnetic wave propagation, radiation, and scattering*, Chapter 3, Prentice-Hal, Inc., 1991.

[16] R. Marques, F. Mesa, M. Horno, "On the correct expansion of leaky modes of planar transmission lines in surface-wave waveguide modes," *1993 European Microwave Conference Digest*, pp. 432-434.